



Kinetics of hydride formation in massive $\text{LaAl}_{0.25}\text{Ni}_{4.75}$ samples

Z. Haberman^{a,*}, J. Bloch^b, M.H. Mintz^{a,b}, I. Jacob^a

^aDepartment of Nuclear Engineering, Ben-Gurion University of the Negev, Beer Sheva 84105, Israel

^bNuclear Research Center-Negev, Beer Sheva 84190, Israel

Abstract

Hydrogen pressures, ranging from 80 to 1 atm, were utilized to study the hydriding kinetics of small, well-shaped $\text{LaAl}_{0.25}\text{Ni}_{4.75}$ samples at temperatures between 246 K and 281 K. The hydrogen absorption was monitored as a function of time at constant temperature and approximately constant pressure. Either a shrinking core (sc) or a low-dimensional nucleation and growth (ng) models fit the experimental data. In one case an interesting feature of thin cracked layer, consisting of bent flakes was revealed in a SEM micrograph of a partly hydrogenated sample. This observation is examined in view of the above models. The pressure dependence of the rate constants indicates an interface-controlled phase transition as the hydride formation rate-determining step. The activation energy for the hydriding process is estimated from Arrhenius plots of the reaction rates to be 0.25 eV/H atom. The results are compared with kinetic data of hydride formation in massive LaNi_5 and powdered $\text{LaAl}_{0.25}\text{Ni}_{4.75}$ samples.

Keywords: Kinetics; Hydride formation; $\text{LaAl}_x\text{Ni}_{5-x}$

1. Introduction

The pseudobinary intermetallic system $\text{LaAl}_x\text{Ni}_{5-x}$, $0 \leq x \leq 1.5$, has been extensively studied in view of its interesting basic and application-oriented properties. These compounds exhibit a broad range of thermodynamic stabilities but their hydrogen absorption capacities significantly decrease toward the Al-rich region [1]. This behavior has been referred as anomalous [2]. Akiba et al. [3] found that “the hydrogen capacity of $\text{LaNi}_{5-x}\text{Al}_x$ ($x \leq 0.25$) was essentially identical...”, and it decreases only for $x > 0.25$. The composition of $x = 0.25$ is also characterized by a softening of the Ni bonding strength as observed in a nuclear resonant photon scattering experiment [4]. The purpose of the present investigation is to study the hydriding kinetics of massive $\text{LaAl}_{0.25}\text{Ni}_{4.75}$ samples. This work comes after a similar kinetic research of LaNi_5 [5] and it is a part of a general attempt to understand some peculiar features of hydrogen absorption in pseudobinary intermetallic systems. The experimental procedure and analysis closely follow those described in more detail in Ref. [5].

2. Experimental

$\text{LaAl}_{0.25}\text{Ni}_{4.75}$ pellets were obtained by melting the pure ($\geq 99.9\%$) metals in an arc furnace. The hexagonal structure and lattice constants ($a = 5.038 \text{ \AA}$, $c = 4.006 \text{ \AA}$) were confirmed by X-ray diffraction. Parallelepiped samples of masses up to 100 mg were cut from the pellets and placed in a copper-made holder which was introduced into a stainless steel system. The hydriding kinetics were recorded under approximately constant pressures and temperatures. The experimental conditions are summarized in Table 1. Scanning electron microscope (SEM) was used to take ex-situ micrographs of partially hydrided samples. More experimental details may be found in Refs. [5–7].

3. Results and analysis

The hydriding kinetic rates at different temperatures were compared at approximately constant (usually less than $\pm 10\%$) p/p_e ratios, as suggested by Goudy and coworkers [8,9]. The equilibrium pressures, p_e , at the temperatures employed in the present work were estimated by utilizing interpolated heat of formation, ΔH ($-8.5 \text{ kcal/mol H}_2$), and entropy of formation, ΔS ($-27.5 \text{ cal}/(^{\circ}\text{K}\cdot\text{mol H}_2)$) [1].

*Corresponding author.

Table 1
Summary of the experimental conditions and results

No.	Mass (mg)	Dimensions (mm)	p/p_e	p (atm)	T (K)	K_{sc} (1/min)	E_a (eV/H at.)	K_{ng} (1/min)	E_a (eV/H at.)
1	31	1.5×1.6×1.7	75	2.5	246	0.0978	0.25±0.02	0.288	0.24±0.02
2	33	1.3×1.6×1.9				0.0863		0.258	
3	39	1.5×1.6×2.0				0.0668		0.196	
4	21	1.3×1.4×1.7		5	259	0.121		0.362	
5	28	1.5×1.5×1.7				0.109		0.325	
6	29	1.3×1.7×1.9				0.161		0.487	
7	30	1.4×1.7×1.7				0.173		0.521	
8	34	1.3×1.7×2.1		10.5	272	0.208		0.618	
9	49	1.3×2.1×2.3				0.247		0.728	
10	60	2.0×2.0×2.1				0.204		0.612	
11	29	1.3×1.8×1.8		17	281	0.268		0.793	
12	45	1.7×1.8×2.0				0.446		1.306	
13	45	1.7×1.8×2.1				0.354		1.038	
14	91	2.0×2.1×3.2				0.409		1.207	
15	34	1.5×1.8×1.9	140	4.5	246	0.0934	0.25±0.02	0.279	0.25±0.02
16	40	1.1×2.3×2.3				0.103		0.301	
17	69	1.7×2.3×2.3				0.0999		0.298	
18	27	1.4×1.5×1.6		9.5	259	0.190		0.559	
19	36	1.5×1.6×1.8				0.209		0.612	
20	42	1.7×1.8×1.8				0.172		0.514	
21	44	1.7×1.8×2.0		20.5	272	0.371		1.097	
22	49	1.7×1.8×2.3				0.287		0.852	
23	64	1.3×2.0×3.6				0.333		1.001	
24	92	1.8×2.1×3.2				0.354		1.039	
25	38	1.6×1.7×2.1		33.5	281	0.386		1.146	
26	39	1.4×2.0×2.0				0.530		1.562	
27	45	1.4×2.0×2.3				0.497		1.488	
28	67	2.1×2.1×2.1				0.391		1.166	
29	29	1.5×1.6×1.9	340	11	246	0.122	0.25±0.02	0.358	0.25±0.02
30	68	1.8×2.3×2.3				0.129		0.385	
31	38	1.6×1.6×2.3				0.098		0.295	
32	40	1.4×1.9×2.1				0.117		0.351	
33	23	1.2×1.4×1.8		23.5	259	0.189		0.559	
34	31	1.4×1.7×1.8				0.217		0.641	
35	33	1.4×1.8×2.0				0.229		0.687	
36	10	0.8×0.9×2.0		50.5	272	0.399		1.187	
37	20	1.2×1.2×2.2				0.362		1.064	
38	32	1.4×1.8×1.8				0.355		1.057	
39	25	1.4×1.5×2.3		81	281	0.417		1.253	
40	25	1.2×1.7×1.8				0.493		1.470	
41	28	1.4×1.6×1.6				0.590		1.790	
42	36	1.5×2.0×2.1				0.509		1.527	
43	19	1.1×1.4×1.6	43	1.3	246	0.0642		0.191	
44	36	1.2×1.7×2.4				0.0402		0.119	
45	73	1.7×2.1×2.7				0.0705		0.212	
46	21	1.1×1.3×1.9	490	15		0.122		0.310	
47	25	1.4×1.6×2.3				0.0989		0.295	
48	31	1.4×1.6×1.9				0.104		0.355	

T is the temperature, p is the applied pressure, p_e is the estimated equilibrium plateau pressure at the relevant temperature, K_{sc} and K_{ng} are the reaction rate constants for the shrinking core and the nucleation and growth models, respectively. E_a is the activation energy.

Typical time-dependent experimental absorption curves are shown in Fig. 1. All hydriding kinetics obtained in this work disclose a good fit with the shrinking core (sc) $F_{sc}(\alpha)$ function, e.g., [10,11], depending linearly on the time, t :

$$F_{sc}(\alpha) = 1 - (1 - \alpha)^{1/3} = ut/r \quad (1)$$

α is the reacted fraction of the metal, u is the velocity of the advancing hydride front and r is a linear dimension of the shrinking particle (a cube of side $2r$ or a sphere of radius r). Analysis (Fig. 2) of Eq. (1) provides the reaction rate constants $K_{sc} = u/r$ for the shrinking core model.

It was found that the kinetic results fit also well a

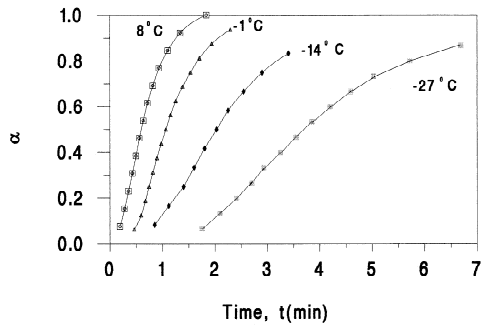


Fig. 1. Time-dependent hydrogen absorption curves for $\text{LaAl}_{0.25}\text{Ni}_{4.75}$ samples of masses 45 mg, 64 mg, 42 mg, 69 mg at temperatures 8 °C, -1 °C, -14 °C, -27 °C, respectively. The reacted metal fractions $\alpha(t)$ at time t were measured at pressure ratio $p/p_e \approx 140$.

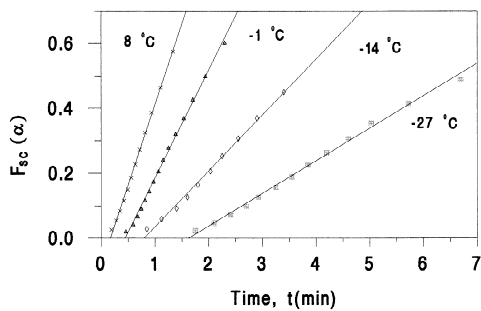


Fig. 2. A linear time-dependence of the shrinking core $F_{sc}(\alpha)$ function for the samples and conditions presented in Fig. 1.

low-dimensional nucleation and growth (ng) model, which is characterized by the following F_{ng} function [10,11]:

$$F_{ng}(\alpha) = [-\ln(1 - \alpha)]^{1/n} = K_{ng}t \quad (2)$$

The exponent n is associated with the dimensionality of growth and with the nucleation rate per unit volume [12]. The present results fitted best $n=1.5$. K_{ng} is the reaction rate constant for the ng model, and is associated with the geometry of the growing nuclei, the initial number of

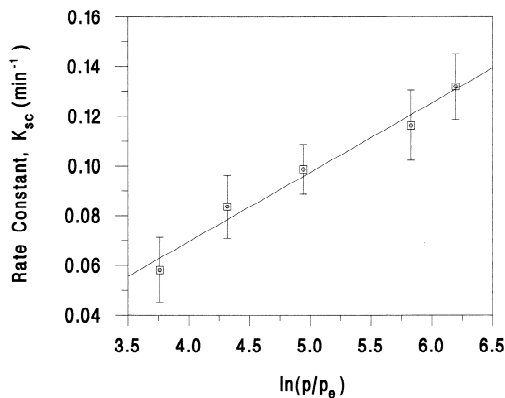


Fig. 3. A linear dependence of the K_{sc} rate constant at -27 °C on the logarithm of the pressure ratio p/p_e .

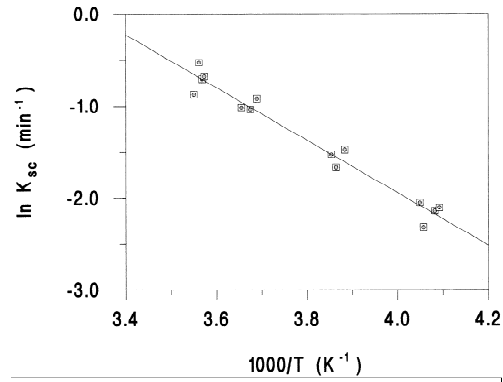


Fig. 4. A semilogarithmic (Arrhenius) plot of the K_{sc} hydriding rate constant vs. the reciprocal absolute temperature $1/T$ for pressure ratio $p/p_e \approx 340$. The slope of the fitted straight line is proportional to the activation energy, E_a .

nuclei per unit volume, the growing velocity of the nuclei and the dimensionality of growth.

The reaction rate constants, K_{sc} and K_{ng} , depend on the applied hydrogen pressure at all the measured temperatures. The highest p/p_e ratio of approximately 500 was attained at 246 K (Table 1). It appears that there is a linear correlation between K_{sc} (Fig. 3) or K_{ng} and $\ln p/p_e$. Arrhenius plots of $\ln K_{sc}$ and $\ln K_{ng}$ vs. the reciprocal temperature $1/T$ determine the activation energy, E_a , of the hydriding process to be $E_a/k_B = E_a/R = (2875 \pm 200)$ K, where k_B is the Boltzmann constant and R is the ideal gas constant (see Fig. 4 Table 1). Our results indicate that the apparent activation barriers can be evaluated without an explicit knowledge of the controlling mechanism [13].

Partly hydrided $\text{LaAl}_{0.25}\text{Ni}_{4.75}$ samples, taken out of the hydrogenation system even in the very initial stages of the hydrogen absorption always exhibited fragmentation to smaller particles and powder. A SEM micrograph of a partly hydrided sample shows an interesting feature in the form of a cracked layer consisting of bent flakes, which are

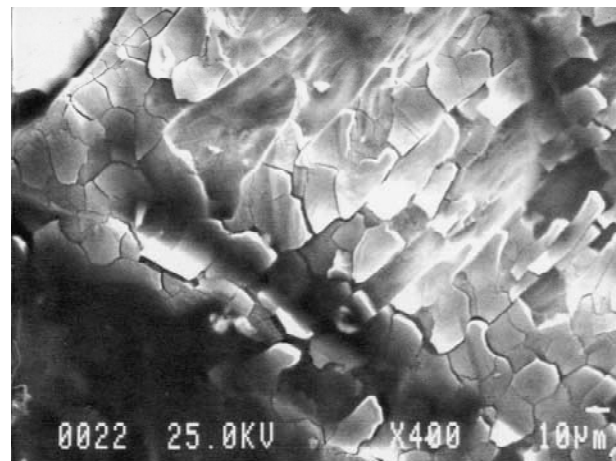


Fig. 5. SEM micrograph of a partly hydrided $\text{LaAl}_{0.25}\text{Ni}_{4.75}$ sample reveals a thin, cracked outermost layer that is peeling off.

peeling off the surface (Fig. 5). This structure resembles a disjoin of the surface of soil dried by the sun.

4. Summary and discussion

The inability to examine partly hydrided one-piece samples made an unambiguous determination of the hydriding kinetic mechanism impossible. However the features revealed in Fig. 5 may shed some light on the hydrogenation process. It is obvious that the blurry structure observed in partly hydrided LaNi_5 (Fig. 5 of Ref. [5]) and the present features in Fig. 5 expose akin characteristics. To the best of our knowledge, such patterns of hydride formation have not been observed previously. There are two possibilities to explain the appearance of this type of structure. One is that a network of hydrides is formed along the flakes borders. The dilation occurring in this region causes the detachment and bending observed in this structure. The conclusion of Kim et al. [14] about the LaNi_5H_x nucleation and growth as thin plates or needles should be mentioned in this context. This is consistent with low-dimensional nucleation and growth and with the $n = 1.5$ exponent in Eq. (2). The second possibility is that this structure forms when the sample is taken out of the hydrogenation system (for SEM analysis). Decomposition of the hydride starts at the surface and results in a shrinkage of the outermost layer. This shrinkage causes the cracking and bending pattern characteristic of dried soil. In any case this structure may be considered as a fingerprint of a previously existing thin hydride layer. This is consistent with the fit to a sc model.

The linear dependence of the reaction rate constants on the logarithms of the applied H_2 pressure implies [15] a metal–hydride phase transformation as the rate-limiting step. The value of 2875 K, derived for E_a/k_B or E_a/R , yields 0.25 eV/H atom or 24.1 kJ/g at H in terms of the reacting hydrogen atoms. This E_a value is lower than the one obtained for the hydride formation in massive LaNi_5 [5]. This trend correlates nicely with the observed softening of the Ni bonding strength in $\text{LaAl}_{0.25}\text{Ni}_{4.75}$ [5]. On the contrary, an increase of the hydriding activation energy with x has been observed in $\text{LaAl}_x\text{Ni}_{5-x}$ by other investigators [9,16], who have however performed the kinetic experiments with well-cycled activated powders [9,16].

In summary, we have measured the hydriding kinetics of massive $\text{LaAl}_{0.25}\text{Ni}_{4.75}$ samples of defined geometrical

shape over a wide range of pressures and temperatures. The pressure dependence of the hydriding rate constants indicates an interface-controlled hydride formation, while their temperature variation yields the activation energy of the process. A SEM picture of cracked layer in partly hydrided sample has been obtained. The inspection of this picture substantiates to some extent the sc and low-dimensional ng models that fit the time dependence of the hydrogen absorption process.

Acknowledgments

This work was supported by a grant of the Israeli Council of Higher Education and the Israeli Atomic Energy Commission.

References

- [1] M.H. Mendelsohn, D.M. Gruen and A.E. Dwight, *Nature*, 269 (1977) 45.
- [2] K. Gschneidner, Jr., T. Takeshita, Y. Chung and O.D. McMasters, *J. Phys. F*, 12 (1982) L1.
- [3] E. Akiba, H. Hayakawa, Y. Ishido, K. Nomura, S. Shin and T. Minesawa, *Mater. Res. Soc. Meet. on Advanced Materials*, Vol. 2, MRS, Pittsburgh, PA, 1989, p. 39.
- [4] I. Jacob, O. Shahal, R. Moreh, A. Wolf and Z. Gavra, *Phys. Rev. B*, 38 (1988) 7806.
- [5] A. Osovizky, J. Bloch, M.H. Mintz and I. Jacob, *J. Alloys Comp.*, 248 (1997) 209.
- [6] N. Bronfman, J. Bloch, M.H. Mintz, D. Sarussi and I. Jacob, *J. Alloys Comp.*, 177 (1991) 183.
- [7] D. Sarussi, I. Jacob, J. Bloch, N. Shamir and M.H. Mintz, *J. Alloys Comp.*, 191 (1993) 91.
- [8] A.J. Goudy, D.G. Stokes and J.A. Gazzilo, *J. Less-Common Met.*, 91 (1983) 149.
- [9] J.T. Koh, A.J. Goudy, P. Huang and G. Zhou, *J. Less-Common Met.*, 153 (1989) 89.
- [10] J.H. Sharp, G.W. Brindley and B.N. Naharari Achar, *J. Am. Ceramic Soc.*, 49 (1966) 379.
- [11] J.D. Hancock and J.H. Sharp, *J. Am. Ceramic Soc.*, 55 (1972) 74.
- [12] J.W. Christian, *The Theory Of Transformations in Metals and Alloys, Part I, Equilibrium and General Kinetic Theory*, Pergamon, Hungary, 1975.
- [13] P.C. Kapur, *J. Am. Ceramic Soc.*, 56 (1973) 79.
- [14] G. Kim, C. Chun, S. Lee and J. Lee, *Acta Metall. Mater.*, 42 (1994) 3157.
- [15] T.B. Flanagan, in A.F. Andresen and A.J. Maeland (eds.), *Hydrides for Energy Storage*, Pergamon Press, Oxford, 1978, p. 135.
- [16] X.L. Wang and S. Suda, *J. Less-Common Met.*, 191 (1993) 5.